Available online at www.sciencedirect.com

ScienceDirect

Biomedical Journal

journal homepage: www.elsevier.com/locate/bj

Original Article

A quantitative validation of segmented colon in virtual colonoscopy using image moments

K.N. Manjunath [a,*], *G.K. Prabhu* [b], *P.C. Siddalingaswamy* [a]

[a] *Computer Science & Engineering, Manipal Institute of Technology, Manipal Academy of Higher Education, Manipal, India*
[b] *Electronics and Communication, Manipal University, Jaipur, 303007, India*

ARTICLE INFO

Article history:
Received 27 September 2018
Accepted 10 July 2019
Available online 25 February 2020

Keywords:
Euclidean space
Colon segmentation
Quantitative analysis
Spatial features
Volumetric overlap

ABSTRACT

Background: Evaluation of segmented colon is one of the challenges in Computed Tomography Colonography (CTC). The objective of the study was to measure the segmented colon accurately using image processing techniques.

Methods: This was a retrospective study, and the Institutional Ethical clearance was obtained for the secondary dataset. The technique was tested on 85 CTC dataset. The CTC dataset of 100–120 *kVp*, 100 mA, and ST (Slice Thickness) of 1.25 and 2.5 mm were used for empirical testing. The initial results of the work appear in the conference proceedings. Post colon segmentation, three distance measurement techniques, and one volumetric overlap computation were applied in Euclidian space in which the distances were measured on MPR views of the segmented and unsegmented colons and the volumetric overlap calculation between these two volumes.

Results: The key finding was that the measurements on both the segmented and the unsegmented volumes remain same without much difference noticed. This was statistically proved. The results were validated quantitatively on 2D MPR images. An accuracy of 95.265±0.4551% was achieved through volumetric overlap computation. Through *paired t − test*, at $\alpha = 5\%$, statistical values were $p = 0.6769$, and $t = 0.4169$ which infer that there was no much significant difference.

Conclusion: The combination of different validation techniques was applied to check the robustness of colon segmentation method, and good results were achieved with this approach. Through quantitative validation, the results were accepted at $\alpha = 5\%$.

* *Corresponding author*. Computer Science & Engineering, Manipal Institute of Technology, Manipal Academy of Higher Education, Tiger Circle Rd., Madhav Nagar, Manipal, Karnataka 576104, India

E-mail address: knm_mit@yahoo.com (K.N. Manjunath).

Peer review under responsibility of Chang Gung University.
https://doi.org/10.1016/j.bj.2019.07.006

At a glance of commentary

Scientific background on the subject

CT Colonography is a new noninvasive medical imaging technology for the analysis of colon polyps using computer software. Accuracy of polyp measurement is completely dependent on the accuracy of colon segmentation. Most of the segmentation techniques are application-specific, and it is difficult to achieve a ubiquitous solution.

What this study adds to the field

Volumetric measurement of any anatomy is the tough task before the radiologist either before segmentation or thereafter. The contribution in this work helps in measuring the segmented colon more accurately in 3D space through three different approaches. This helps in accurate colon polyp analysis.

CT Colonography is a new non-invasive technology for the analysis of colon polyps using computer software. Accuracy of polyp measurement is completely dependent on the accuracy of colon segmentation. Most of the segmentation techniques are application specific, and it is difficult to achieve a ubiquitous solution. The question arises about the accuracy of the results. Validation of results is a tough task where the accuracy is less in the present state-of-the-art software [1]. The segmented colon is checked either manually on 2D MPR (Multi-Planar Reformatted) image plane or through quantitative assessment methods to know the quality of the results and several colon segmentation techniques with different validation methods employed to assess the results exist there. To know the extent of the work done in this problem domain, a detailed literature review comprising articles from the technical and medical point of view was considered.

Punwani [2] worked on the assessment of colonic segment movement in both the supine and the prone positions. They inferred that the inaccurate colon segmentation could lead to variation in the polyp assessment. In a study [3], the smaller polyps were underestimated in CTC due to inaccurate segmentation. Even though the polyp measurements were validated clinically there hardly exists any literature that talks about the validation of the segmentation results [1]. The lack of these techniques is also one of the reasons why the computer methods of colon assessment are not widely accepted [4,5]. Taylor et al. [6] studied on colon distention with the aid of different oral contrasts. The authors suggested that a complete solution of colon segmentation and its quantitative assessment could reduce the burden on the radiologist. Gerig et al. [7] developed a tool for quantitative evaluation of 3D structures. The tool included percentage overlap of segmented structures and mean/median absolute distances between the object surfaces and the maximum (Hausdorff) distance. A colon segmentation technique based on the geometrical features of the colon is discussed in Ref. [8] – only the qualitative validation is discussed.

The objective of our study is to address these issues providing an efficient method to validate the segmented colon accurately. In this paper, three-volume measurement techniques are discussed and the results are proved through qualitative and quantitative analysis.

Materials and methods

The CT Colonography dataset was downloaded from The Cancer Imaging Archive (TCIA), USA [9–11]. The images were of good diagnostic quality and were acquired with the standard CTC protocol ACRIN 6664 [12]. Empirical testing includes eighty-five samples ($n = 85$) of good diagnostic quality images. The imaging parameters were, 8 slices MDCT images, Feet First Supine and Feet First Prone position scans, ST (Slice Thickness) $= 1.25mm$ *and* $2.5mm$, $imageresolution = 512 \times 512$, ~1000 images/patient, $mA = \{200 - 300\}$, 120 kVp and $age = \{40..80\}$ years acquisitioned from SIEMENS Somatom™ (SIEMENS Healthcare, Erlangen, Germany). The authenticity of the images was checked through DICOM [13,14] validation framework that we had implemented.

The proposed methodology is illustrated in Fig. 1. After CT image acquisition, the 3D volume is constructed in R^3 dimension from a set of images in R^2 and the colon is segmented and visualized with object-based visualization techniques. The statistical property of the segmented colon (moments) is calculated and analyzed in three different ways using the statistical analysis.

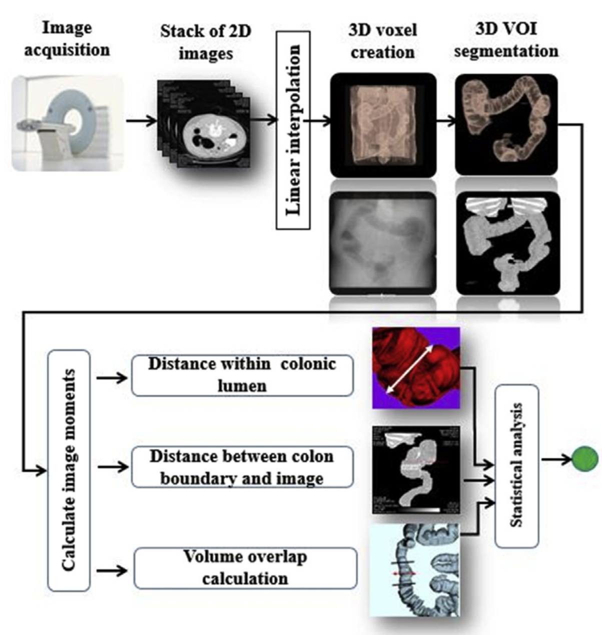

Fig. 1 Illustration of the colon segmentation, distance measurement, and the validation techniques.

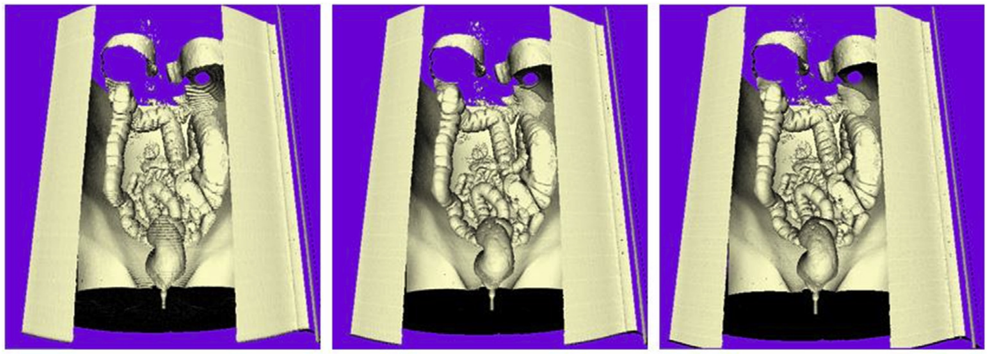

A B C

Fig. 2 3D volume visualized through surface rendering technique with thick and thin slices. (A) 3.0 mm, (B) 1.5 mm, and (C) 0.75 mm. Thicker slices produce a kind of staircase effect and not the smooth transition in z-axis.

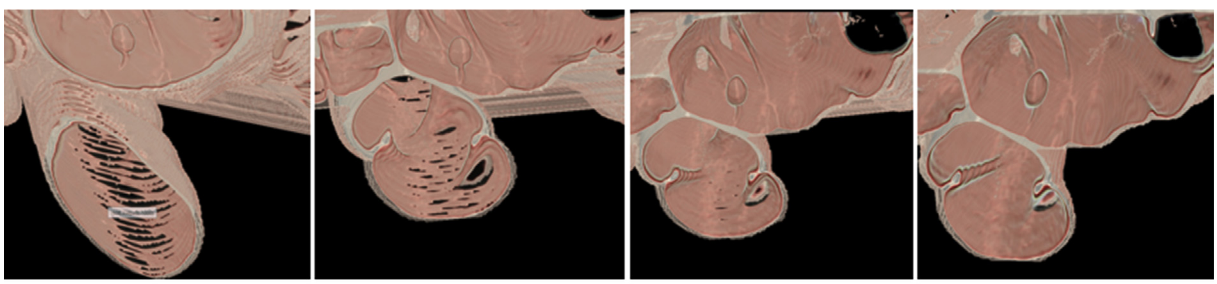

A B C D

Fig. 3 A segmented colon visualized through direct volume rendering technique with variable slice thickness to demonstrate the staircase effect in the case of higher slice thickness. (A) 5.0 mm (stair case effect can be observed), (B) 3.0 mm, (C) 1.5 mm, and (D) 0.75 (there is no discontinuity in the colon boundary also). Improvement in the results can be observed when moved from thick to thin slices.

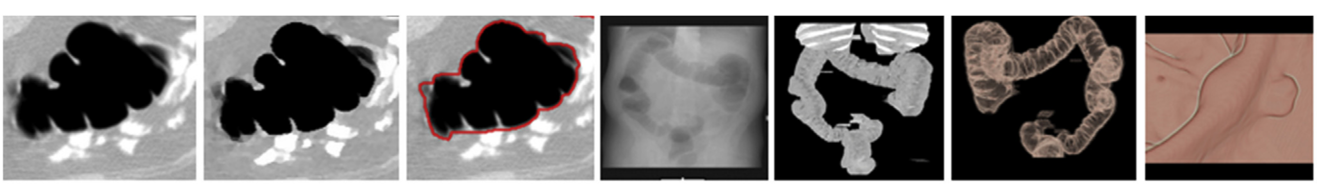

A B C D E F G

Fig. 4 The results of colon segmentation are presented systematically. (A) Unprocessed axial slice, (B) Noise reduction with adaptive smoothing, (C) Colonic segment boundary delineation, (D) DRR of unsegmented colon in Anterior to Posterior (AP) view, (E) DRR of segmented colon, (F) The volume rendered image of segmented colon and (G) The endoluminal view after segmentation.

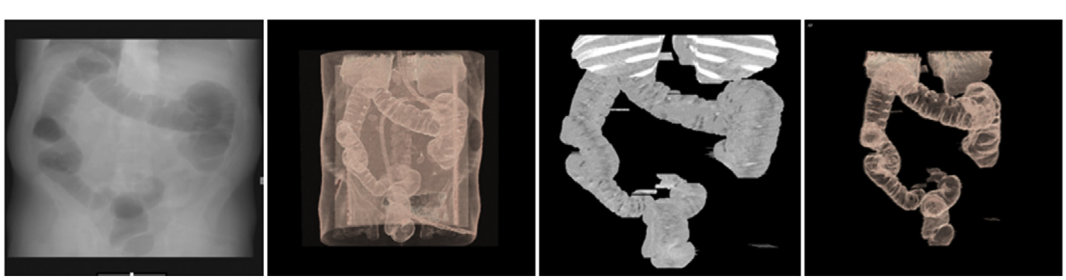

A B C D

Fig. 5 Object-based renderings in anterior to posterior direction used for validation. (A) An Un-segmented DRR, (C) First voxel hit of segmented colon, (B, D) Direct volume rendering of un-segmented and segmented colon, respectively.

Calculation

Volume reconstruction

Before segmenting the Volume of Interest (VOI), the 2D slices are preprocessed with *contrast correction* and *gamma correction*, and then the volume is reconstructed in 3D through *linear interpolation*. The Gamma correction, which decodes the stored pixel value in DICOM file to its actual displayable quantity [15], is applied. When the same image looks different in different display systems [16,17] without decoding it may lead to wrong clinical interpretation. The preprocessed image quality is compared with the image viewers' syngo FastView™ [18] and the ImageViewer™. Due to the unequal size of the pixel in x and y direction, the linear interpolation technique is applied to create *isotropic voxels*. With this, a smooth transition is noticed near the surface of the structures when compared to

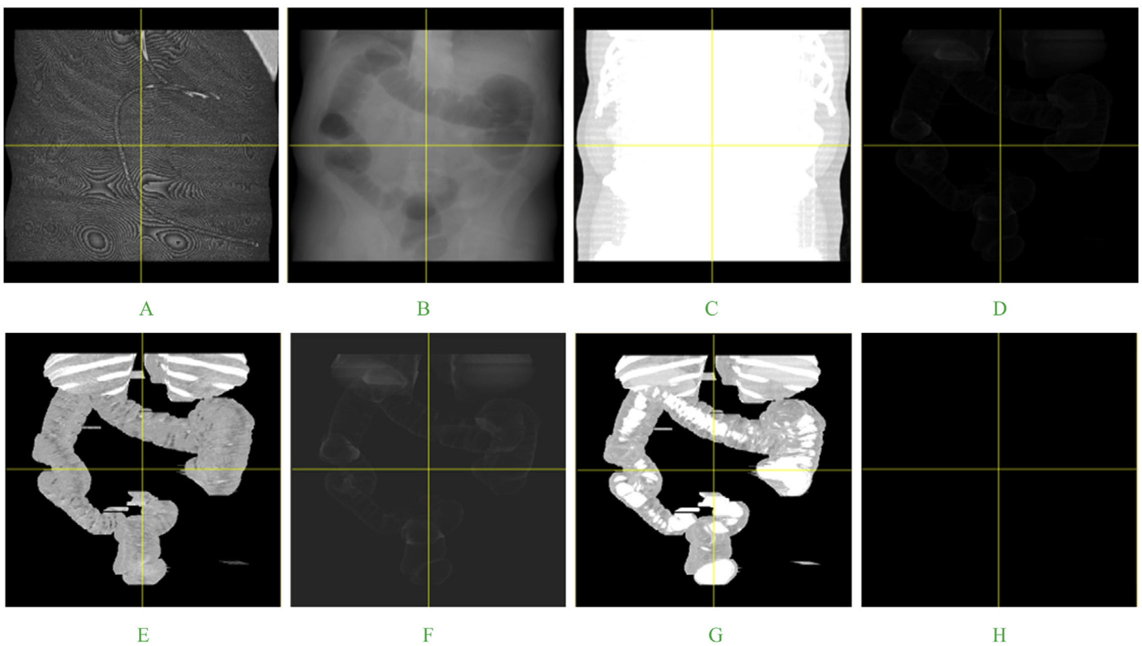

Fig. 6 Different object-based visualization methods (row 1 – before colon segmentation and row 2 – after colon segmentation in anterior to posterior direction). (A, E) First voxel hit, (B, F) Digitally reconstructed Radiograph, (C, G) Maximum Intensity Projection, and (D, H) Minimum Intensity Projection.

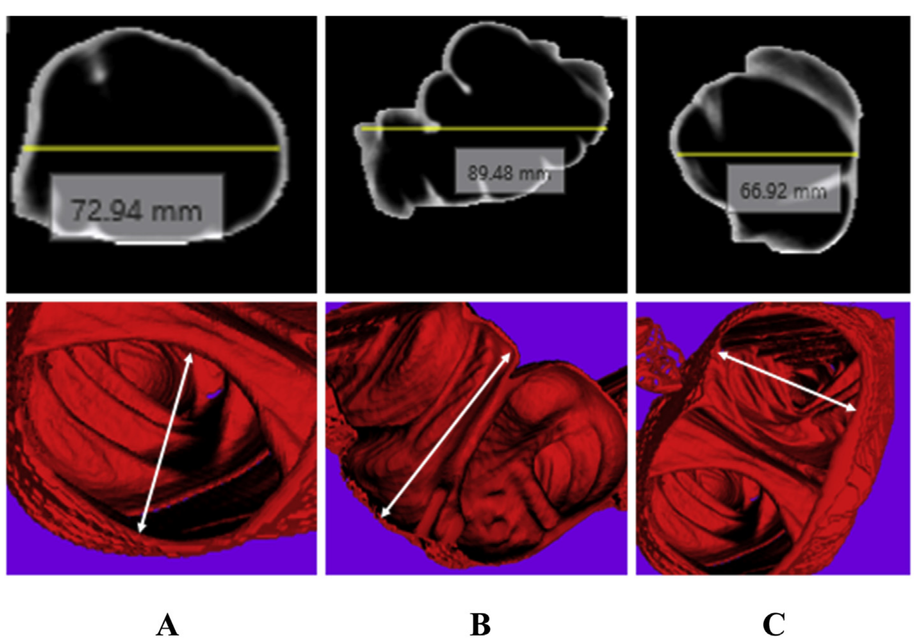

Fig. 7 Intra lumen distance measures shown on axial MPRs (row 1) and surface rendered images (row 2). (A) Distance in transverse colon. (B) In hepatic flexure and (C) In splenic flexure.

the higher *ST* [Fig. 2C]. The slices with higher *ST* are interpolated to 0.625 *mm* based on the size of the pixels, which are in the range {0.546875 − 0.9765625*mm*}. Fig. 2 shows the surface rendering of the unsegmented patient volume at variable *ST*. With the higher *ST*, a staircase effect, which does not show smooth transition of anatomies [Fig. 2A], can be observed. The images used for 3D volume reconstruction in Fig. 2 were acquired with 0.75 mm slice thickness (2000 CT images in a dataset). As it is not possible to expose the patient again to the radiation just to get the images with different slice thicknesses, for demonstration purpose we simulated this surface rendering with a variable ST by skipping the intermediate slice in Fig. 2B (reduced to 1000 slices) and 2A (reduced to 500 slices). In addition, the original number of slices can be reconstructed again as it is from these new sets of images through interpolation. Fig. 3 shows the direct volume rendering of the colon interior at variable *ST*. As moved towards the higher *ST*, the segmentation may lead to boundary leak problems [Fig. 3A] and may not give the accurate measurements. This suffices that without an interpolation technique, there are chances of inaccurate measurements of unequal voxel sizes.

Current state-of-the-art CT scanners produce the pixels of square shape. All the dataset in this study were acquired with the latest CT scanners such as SIEMENS Somatom Session™, Philips Brilliance™ and Toshiba Aquilion™. As per the DICOM conformance statement of these products, these scanners produce the pixels of square shape. Due to this, to achieve the voxel of equal size in all three directions of patient coordinate

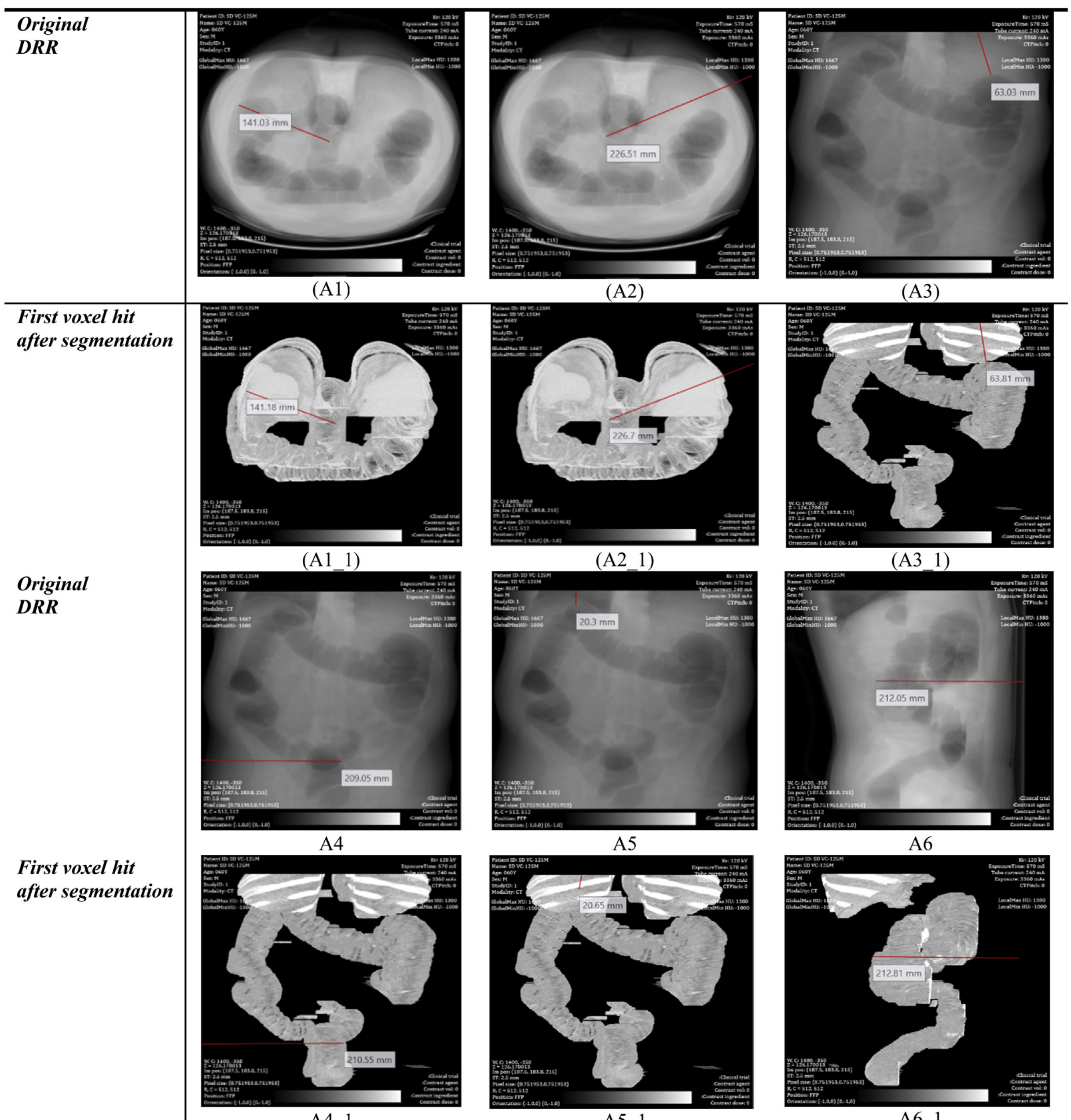

Fig. 8 Distance measured on DDR and first voxel hit of unsegmented and segmented volumes.

Table 1 Distances measured. Column D: On DRR image of unsegmented colon. Column E: On DRR image of segmented colon.

Sl. no.	Dataset	Orthogonal plane	$x_i \epsilon mm$	$y_i \epsilon mm$
1	Sample 1	Axial	119.57	119.1
2	Sample 1	Axial	141.03	141.18
3	Sample 1	Axial	226.51	226.7
4	Sample 1	Axial	292.52	293.27
5	Sample 1	Coronal	63.03	63.81
6	Sample 1	Coronal	20.3	20.65
7	Sample 1	Coronal	209.05	210.55
8	Sample 1	Coronal	226.34	226.35
9	Sample 1	Sagittal	212.05	212.81
10	Sample 1	Sagittal	162.47	162.51
11	Sample 1	Sagittal	26.49	26.36
12	Sample 1	Sagittal	221.09	221.85
13	Sample 2	Coronal	45.36	45.12
14	Sample 2	Coronal	320.05	320.14
15	Sample 2	Axial	134.34	134.11
16	Sample 3	Axial	234.12	234.56
17	Sample 4	Coronal	54.54	54.12
18	Sample 5	Sagittal	189.98	190.55
19	Sample 5	Axial	232.01	231.34
20	Sample 6	Axial	236.43	236.0
21	Sample 7	Coronal	34.12	33.45
22	Sample 7	Coronal	78.34	77.65
23	Sample 8	Coronal	89.91	89.78
24	Sample 9	Sagittal	176.05	176.59
25	Sample 9	Sagittal	109.89	109.12
26	Sample 9	Axial	312.4	311.2
27	Sample 10	Coronal	45.90	45.12
28	Sample 10	Sagittal	134.12	133.4
29	Sample 10	Axial	210.55	211.6
30	Sample 10	Axial	231.2	230.4

system, the linear interpolation technique is applied (also, as only the slice thickness was different in z-axis when compared to the size of the pixel in x and y axis). However, the implementation supports the bilinear also. The testing did not include any such cases with rectangular pixels.

Colon segmentation

After preprocessing, a multi-step boundary based segmentation technique is applied for colon segmentation. It includes recognizing the colonic lumen with adaptive smoothing technique [Fig. 4B], boundary detection with canny operator [Fig. 4C], boundary delineation with Connected Component Labeling [Fig. 4C], and deciding the colonic segments using the prior information of colon distention grading [Fig. 4D] [6,19]. The relationship between the unsegmented volume [Fig. 4E] and the segmented colon [Fig. 4F] is given by Eq. (1), where S is the original 3D volume (V_g), S_o is the segmented colon (V_b) and f, f_0 are the voxel intensities and c is the scene domain. The results are visualized using the object based rendering methods on both the 2D and the 3D views using MPR and direct volume rendering techniques [20].

$$S = (c, f) \rightarrow S_o = (c, f_o) \quad (1)$$

Measurement of segmented volume

Object based visualization methods [Fig. 6A–D] are widely used in medical imaging applications for validating the segmentation results. Examples are maximum intensity projection (MaxIP), minimum intensity projection (MinIP), first voxel hit and averaging (i.e. digitally reconstructed radiographs - DRR). These images can be generated in any direction of patient coordinate system (PCS). For example, DRR is used for registering the 2D x-ray image with the DRR image generated from 3D volume for position accuracy in the case of radiation therapy workflow. In this work, on 2D MPR, the *DRR* of the unsegmented colon and first voxel hit of segmented colon are used for measuring the distance in Euclidean space (Eq. (2)). The DRR and the first voxel hit images show the anatomy distribution of a 3D volume on a 2D image. This helps in measuring the segmented volume accurately in the required viewing direction. Fig. 5A shows the distribution of large intestine in *AP* direction on a DRR image. The evaluation of the segmented VOI is implemented on DRR in three different ways. In all the cases, the distance is measured on *axial*, *sagittal*, and *coronal* views. The measurement and the results were validated through qualitative analysis by an expert radiologist. Only one observer's decision was considered, as the multiple readers' evaluation might not have impact [2,21,22].

$$d(u, v) = \sqrt{(u.X - v.X)^2 + (u.Y - v.Y)^2 + (u.Z - v.Z)^2} \quad (2)$$

The first voxel hit method draws the 2D picture from the 3D volume as and when the first voxel is encountered by the projection ray and the method stops piercing the 3D volume further. With this, it just gives the boundary details of the outer surface [Fig. 6A] and not the depth information of the

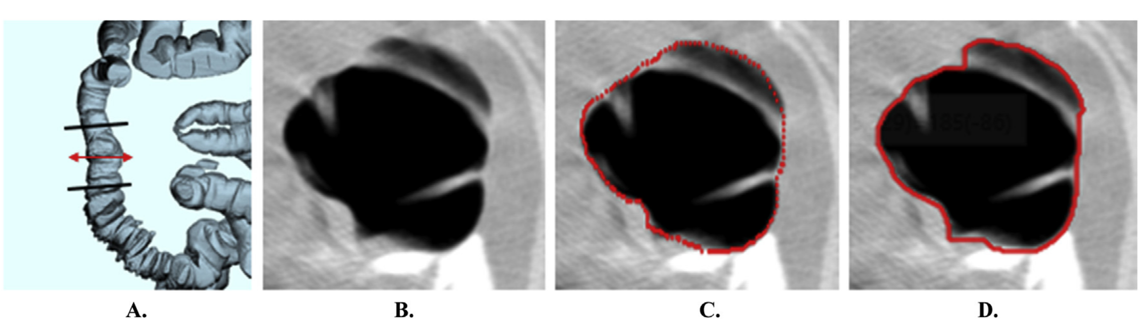

Fig. 9 Volumetric overlap computation in the subset of volume. (A) The subset of slices considered, (B) The original axial slice showing the cross-sectional segment of the colon, (C) Manually drawn contour points, and (D) Boundary points delineated through the automated colon segmentation technique.

anatomy [Fig. 6B] when applied on unsegmented colon whereas this method gives a proper visualization of the anatomy after the segmentation [Fig. 6E]. MaxIP gives the maximum of the voxel intensity along the projection rays. In case the anatomy has higher voxel intensities (>2000HU let us say) due to bone [Fig. 6C] or metal implant or due to oral contrast medium [Fig. 6G], it always gives the higher intensity values by skipping the intensities of the tissues [Fig. 6C]. MaxIP is applicable only in case when hard structures visualization is required. MinIP is exactly similar to MaxIP, but it projects the minimum intensity instead of maximum. As the tubular structure of colon has either air or CO_2 inside the lumen, it appears black on the MPR images (its voxel intensity is < -900 HU or 0 gray value when displayed with specific window value). The minIP method always gives voxels in the dark region due to which it is very difficult to visualize the colon on 2D MPR [Fig. 6D, H]. All these methods are equally good, but they are application specific and in this context of colon analysis, the DRR of unsegmented colon and the first voxel hit of segmented colon have given good results when compared to MaxIP and MinIP.

Measuring intra lumen distance. For the post colon segmentation, the intra lumen distance (between opposite edges) is measured on the axial segment (measures in *mm* are shown in tooltip in Fig. 7) using an electronic caliper. This measure is compared with the geometrical feature (width automatically calculated during CCL) of the colonic segment on the corresponding slice. This is repeated for fifty slices. A significant difference between these two measures is determined using $paired\ t-test$ method. The measurements remain the same. The first row in Fig. 7 shows the distance measured on axial MPR in hepatic flexures segment of colon and the second row shows the surface rendered image with Marching cube algorithm [23]. The double-headed arrow in row 2 illustrates the opposite sides of the colon – the distension of the ascending colon.

Distance between field of view and colonic segments in arbitrary direction. Similar to the previous technique, the distance is measured from the field of view (image boundary) to the colonic segments on a DRR image of the unsegmented and the first voxel hit image of the segmented colon. This feature helps to locate the position of colon from the periphery of the abdomen. Different cases are shown in Fig. 8. The measurements are distance between the rectum and the descending colon [Fig. 8A1], volume boundary to the recto sigmoid junction [Fig. 8A2], beginning of CT scan area to hepatic flexure [Fig. 8A3], from volume boundary to the recto sigmoid junction in lateral direction [Fig. 8A4], from the CT couch top to the top of the transverse colon [Fig. 8A5] and from the patient skin to the front of the transverse colon [Fig. 8A6]. This technique was applied on eighty-five ($n = 85$) CTC datasets acquired in both the supine and the prone positions. Table 1 shows the measures for 10 patients. Overall 480 measurements ($dof = 479$) were done. The measures are almost same with minor sub-millimeter variation. The distance on DRR of unsegmented volume is considered the Ground Truth (*GT*) and is denoted as x_i. In addition, on the first voxel hit the image is represented as y_i. $paired\ t-test$ was applied to test the difference between x_i and y_i. The mean of differences was equal to 0.0123. In the first group (i.e. x_i), $\overline{\mu_1} = 159.6587$, $\sigma_1^2 = 87.0135$, $SEM = 3.9716$, in group 2, $\overline{\mu_2} = 159.6463$, $\sigma_2^2 = 87.1539$. The t value at degrees of freedom $dof = 479$ is, $t = 0.4169$, the p value is 0.6769. Since $p > 0.001$, at $\alpha = 5\%$, the small variation in the measures is not significant.

Computing the volume overlap between manually segmented colon and result of the automated method. In the third approach, the boundary points of manually drawn contour (GT) [Fig. 9C] and the automatically segmented colon [Fig. 9D] are compared through *volumetric overlap* (an example of *Image moments*). Since marking the boundary points is tedious for the entire volume and time-consuming, the overlap is calculated (Eq. (3)) for a subset of volume (only for 20 slices as in Fig. 9A). Certain validation techniques in medical imaging are empirically proved considering certain number of samples from the large population and the burden on the radiologist can be reduced to some extent with this approach [24–27]. Here, set A and set B represent the boundary points of the segmentation through GT and the proposed methods, respectively. This is where the computer algorithms outperform in delineating the boundary when compared to the manual methods. The mean of overlap was $\overline{x} = 95.265\%$ with $\sigma = \pm 0.4551\%$ and the accuracy of 95.265±0.4551% was achieved. Other volumetric measurement methods based on surface distance and volume difference are not applied, as they are computationally expensive for the entire volume.

$$Accuracy = \frac{A \cap B}{A \cup B} * 100 \tag{3}$$

In this study, all these distance measurement techniques were applied on CT Colonography images of 512 × 512-image resolution and we got only one high resolution (of 1024 × 1024 resolution) CT dataset. The smoothness of the surface of the structures was far better and we were able to measure the two ends more accurately when compared with the images of lower resolution. It is difficult to defend the better accuracy with high-resolution dataset unless the results are compared with the same patient dataset with lower resolution, let us say 512 by 512. However, the 3D visualization was more visually appealing in high resolution CT. The proposed techniques were tested in a high performance workstation (Intel Core i7® processor, Windows 2010 64 bit HE, 8 GB DDR3 RAM, and NVIDIA GPU).

Conclusion

Existing state-of-the-of-art segmentation techniques lack in accuracy of the results. This is an alternate method in the Euclidean space used to address the problem of accuracy in measurement. It was proved through the statistical analysis showing that the results were acceptable. This technique has to be evaluated on the bulk dataset (at least with $n => 300$) to check its robustness. The measurements went wrong when the voxels of non-uniform sizes were considered and this proves that the voxel with isotropic resolution is necessary during the 3D volume reconstruction. The results cannot be compared with the existing CTC solutions as the dataset and the segmentation techniques used are different. Instead, in an alternate approach, treated an expert radiologist's manually measured values on the DRR of the unsegmented volumes as the ground truth and then compared with the measurements on the first voxel hit method of the segmented volumes achieved through the automated methods. This method can even be applied with the segmentation results of other anatomies based on the clinical need. Testing the method to know the difference when applied on images of different resolutions, measuring the distance between the two voxels on the physical object printed using a 3D printer, and comparing with the software results is the scope for the future work.

Funding

We are grateful to Manipal Academy of Higher Education, Manipal, for supporting this work under Dr. TMA Pai Ph.D. Program.

Conflicts of interest

The authors declare that they have no competing interests.

Acknowledgments

We thank Dr. Rajagopal K V, Radiologist from Department of Radiodiganosis and Imaging, Kasturba Medical College, Manipal for his valuable inputs during implementation. We thank Prof. Shankar Rao, Manipal for English grammer corrections. We extend our thanks to Mr. Yogeesh M (project manager), SIEMENS Healthineers for his consultancy during the design of this research.

REFERENCES

[1] Udupa JK, Herman GT. 3D imaging: principles and approaches. 1999. p. 2–120.

[2] Punwani S, Halligan S, Tolan D, Taylor SA, Hawkes D. Quantitative assessment of colonic movement between prone and supine patient positions during CT colonography. Br J Radiol 2009;82:475–81.

[3] Song B, Zhang G, Lu H, Wang H, Zhu W, Pickhardt PJ, et al. Volumetric texture features from higher-order images for diagnosis of colon lesions via CT colonography. Int J Comput Assist Radiol Surg 2014;9:1021–31.

[4] Cash BD. Establishing a CT colonography service. Gastrointest Endosc Clin N Am 2010;20:379–98.

[5] Pickhardt PJ, Lee AD, Taylor AJ, Michel SJ, Winter TC, Shadid A, et al. Primary 2D versus primary 3D polyp detection at screening CT colonography. AJR Am J Roentgenol 2007;189:1451–6.

[6] Taylor SA, Halligan S, Goh V, Morley S, Bassett P, Atkin W, et al. Optimizing colonic distention for multi-detector row CT colonography: effect of hyoscine butylbromide and rectal balloon catheter. Radiology 2003;229:99–108.

[7] Gerig G, Jomier M, Chakos M. Valmet: a new validation tool for assessing and improving 3D object segmentation. In: Proceedings of international conference on medical image computing and computer-assisted intervention (MICCAI), Utretch; 2010. p. 516–23.

[8] Chowdhury TA, Whelan PF. A fast and accurate method for automatic segmentation of colons at CT colonography based on colon geometrical features. Mach Vis Image Process Conf (IMVIP) Dublin 2011:26–31.

[9] Clark K, Vendt B, Smith K, Freymann J, Kirby J, Koppel P, et al. The cancer imaging archive (TCIA): maintaining and operating a public information repository. J Digit Imaging 2013;26:1045–57.

[10] Smith K, Clark K, Bennett W, Nolan T, Kirby J, Wolfsberger M, et al. CT_COLONOGRAPHY. The Cancer Imaging Archive. 2015. http://doi.org/10.7937/K9/TCIA.2015.NWTESAY1.

[11] Johnson CD, Chen MH, Toledano AY, Heiken JP, Dachman A, Kuo MD, et al. Accuracy of CT colonography for detection of large adenomas and cancers. N Engl J Med 2008;359:1207–17.

[12] ACRIN protocol 6664. American College of Radiology Imaging Network website. 2013. https://www.acrin.org/Portals/0/Protocols/6664/ACRIN_6664_AdminUpdate_080410_master.pdf (Accessed 14 Sept 2018).

[13] The DICOM PS 3.3. DICOM Consortium. NEMA USA website. 2012. http://dicom.nema.org/medical/dicom/current/output/pdf/part03.pdf (Accessed 10 Sept 2018).

[14] DICOM tags. Queens University website. 2017. http://www.sno.phy.queensu.ca/~phil/exiftool/TagNames/DICOM.html. Published 2015. (Accessed 14 Sept 2018).

[15] Erik R, Wolfgang H, Paul D, Sumanta P, Greg W, Karol M. High dynamic range imaging: acquisition, display, and image-based lighting. Massachusetts: Morgan Kaufmann; 2010.

[16] Samei E, Badano A, Chakraborty D, Compton K, Cornelius C, Corrigan K, et al. Executive summary of AAPM TG18 report. Med Phys 2005;32:1205–25.

[17] Kagadis GC, WalzFlannigan A, Krupinski EA, Nagy PG, Katsanos K, Diamantopoulos A, et al. Medical imaging displays and their use in image interpretation. RadioGraphics 2013;33:275–90.

[18] Syngo fast view^{TM} Berlin and Munchen. SIEMENS Healthineers website. 2014. https://www.healthcare.siemens.co.in/medical-imaging-it/syngo-special-topics/syngo-fastview (Accessed 14 Sept 2018).

[19] Slater A, Taylor SA, Burling D, Gartner L, Scarth J, Halligan S. Colonic polyps: effect of attenuation of tagged fluid and viewing window on conspicuity and measurement-in vitro experiment with porcine colonic specimen. Radiology 2006;240:101–9.

[20] Melancon G, Munzer T, Weikopf D. Volume rendering on server GPUs for enterprise scale medical applications. Heidelberg: IEEE Proceedings of symposium on visualization; 2010. p. 1–10.

[21] Jian WX, Suzuki K. Max-AUC feature selection in computer-aided detection of polyps in CT colonography. IEEE J Biomed Health Inform 2014;18:585–93.

[22] Van R, Boellaard TN, Van MP, Serlie IW, Haan MC, Stoker J, et al. Electronic cleansing for 24-h limited bowel preparation CT colonography using principal curvature flow. IEEE Trans Biomed Eng 2013;60:3036–45.

[23] Polygonising a scalar field. Boure P. Website. 2014. http://paulbourke.net/geometry/polygonise (Accessed 19 Sept 2018).

[24] Lee H, Kim B, Lee J, Kim SH, Shin YG, Kim TG. Fold-preserving electronic cleansing using a reconstruction model integrating material fractions and structural responses. IEEE Trans Biomed Eng 2013;60:1546–55.

[25] Li X, Aldridge B, Fisher R, Rees J. Estimating the ground truth from multiple individual segmentations with application to skin lesion segmentation. International Symposium on Biomedical Imaging. Chicago: From Nano to Macro; 2011. p. 1438–41.
[26] Sandberg TH, Nilsson M, Poulsen JL, Gram M, Frøkjær JB, Ostergaard LR, et al. A novel semi-automatic segmentation method for volumetric assessment of the colon based on magnetic resonance imaging. Abdom Imag 2015;40:2232–41.
[27] Perry JP, Joshua B, Jarret K, Jessica BR, Meghan GL, Alejandro MDR, et al. Volumetric analysis of colonic distention according to patient position at CT colonography: diagnostic value of the right lateral decubitus series. Am J Roentgenol 2014;203:W623–8.